Electrical properties of zinc ferrites $Fe_{3-x}Zn_xO_4$ with $0 \leq x < 0.3$

P. Wang,* Z. Kąkol,† M. Wittenauer, and J. M. Honig
Department of Chemistry, Purdue University, West Lafayette, Indiana 47907
(Received 19 March 1990)

Resistivity and Seebeck coefficients are reported in the range 50 K $< T <$ 300 K for zinc ferrite single crystals $Fe_{3-x}Zn_xO_4$ in the composition range $0 \leq x < 0.3$. Samples with $0 < x \lesssim 0.012$ exhibited first-order phase transformations at the Verwey transition; in the range $0.012 < x \lesssim 0.036$ second- or higher-order continuous phase changes were observed. No transitions were encountered for $x \gtrsim 0.036$. The electrical properties of the zinc ferrites are analyzed in terms of hopping charge-carrier transport involving valence fluctuations on cations located on octahedral sites. The electrical properties and Verwey transitions of $Fe_{3-x}Zn_xO_4$ and $Fe_{3(1-\delta)}O_4$ match very well with the compositional correspondence $x \rightleftarrows 3\delta$. Various implications of the above findings are discussed.

INTRODUCTION

We discuss in the following the electrical properties of the zinc ferrite series $Fe_{3-x}Zn_xO_4$ ($0 \leq x < 0.3$). It is of interest to ascertain the changes in conductivity and Seebeck coefficients arising from the systematic substitution of Zn for Fe. Zinc is known to enter the spinel lattice exclusively on tetrahedral interstices; by contrast, the electrical conduction process at and below room temperature is believed to take place by electron transfer among iron ions located at octahedral sites. Thus, considerable interest attaches to the effect of increasing aliovalent substitutions in tetrahedral sites on the electrical characteristics of the zinc ferrites. As far as is known, this problem has not been addressed with electrical measurements on single crystals and therefore remains open.

A second question relates to the alterations in the nature of the Verwey transition that arise from the Zn substitution. As is well documented[1-8] in undoped magnetite, any changes in the oxygen stoichiometry (i.e., alterations of δ in $Fe_{3(1-\delta)}O_4$) produce dramatic effects: For $\delta < \delta_c \approx 0.0039$ the Verwey transition is of first order; for $\delta_c < \delta < 3\delta_c$ it is of second or higher order. Samples with $\delta > 3\delta_c$ cannot readily be produced as single phases because of the proximity of the magnetite, - hematite phase boundary. It is therefore of interest to ascertain whether similar effects can be brought about by increasing the Zn content in zinc ferrites, starting from pure magnetite, and whether the Verwey transition can be entirely suppressed by use of sufficient zinc.

EXPERIMENTAL

The growth of single crystals of

$$Fe_{3-x}Zn_xO_4 \equiv (Fe_3O_4)_{1-x}(Fe_2ZnO_4)_x$$

has been discussed in detail elsewhere.[9] Samples prepared by the skull-melter technique were rendered stoichiometric (i.e., the ideal 4/3 oxygen-to-cation ratio was maintained) by appropriate subsolidus annealing. The samples were also repeatedly checked for uniformity of Zn concentration; the quoted x values were those measured by electron microprobe techniques and energy dispersive x-ray analysis (EDAX), and were roughly 70% of the nominal value. Rectangular parallelepipeds roughly $1 \times 2 \times 10$ mm^3 in dimensions were cut, with the long c axis perpendicular to the large faces. Silver paste was used to attach leads in conventional fashion for four-probe resistivity (ρ) and two-probe Seebeck coefficient (α) measurements. Operational amplifiers were used as buffers. Temperatures were measured by a calibrated carbon glass thermometer. Data were acquired by under computer control; in α measurements the temperature differential between the ends of the sample did not exceed 1 K.

RESISTIVITY MEASUREMENTS

Resistivity measurements over the range 43 to 300 K are shown in Fig. 1(a)–(c) for $Fe_{3-x}Zn_xO_4$ samples with $0 \leq x \leq 0.29$. The detailed changes near the Verwey transition are exhibited in Fig. 2. The following points should be noted.

(1) For the range $0 \leq x \leq 0.035$ all samples exhibit virtually the same temperature variation of resistivity above their respective Verwey transition temperatures ($0 \leq x \leq 0.011$) or above 90 K ($0.014 \leq x \leq 0.035$). By contrast, samples with higher Zn content have distinctive and considerably higher resistivities in the range $90 < T < 300$ K.

(2) Samples with $0 \leq x \leq 0.011$ exhibit a discontinuity in ρ which shrinks in size and moves towards lower temperatures with increasing x [Fig. 1(a)]. As in undoped magnetite (where the assertion could be checked by heat capacity measurements) this is taken to reflect the occurrence of a first-order Verwey transition at the temperature T_V. Samples with $0.014 \leq x \leq 0.035$ exhibit an inflection point in the $\log_{10}\rho$ versus $1/T$ dependence, as indicated by the arrows in Fig. 2. The location of these arrows is virtually identical with the inflection points encountered in plots of ρ versus T. This is taken to reflect the occurrence of a second- (or higher-) order, i.e., continuous, Verwey transition in the above range of composition. For zinc ferrite with $x = 0.035$ the second-order

transformation is barely detectable. In the composition range $0.13 \leq x \leq 0.29$ the electrical characteristics are completely altered. There is no transition, only a gentle variation in the $\log_{10}\rho$ versus $1/T$ plots; the curves in Fig. 1(c) are much flatter than those of Figs. 1(a) or 1(b). The three curves intersect at a common temperature of ≈ 90 K and the communality of the $\rho(T)$ dependence above 100 K encountered for samples with $x \leq 0.035$ has been lost.

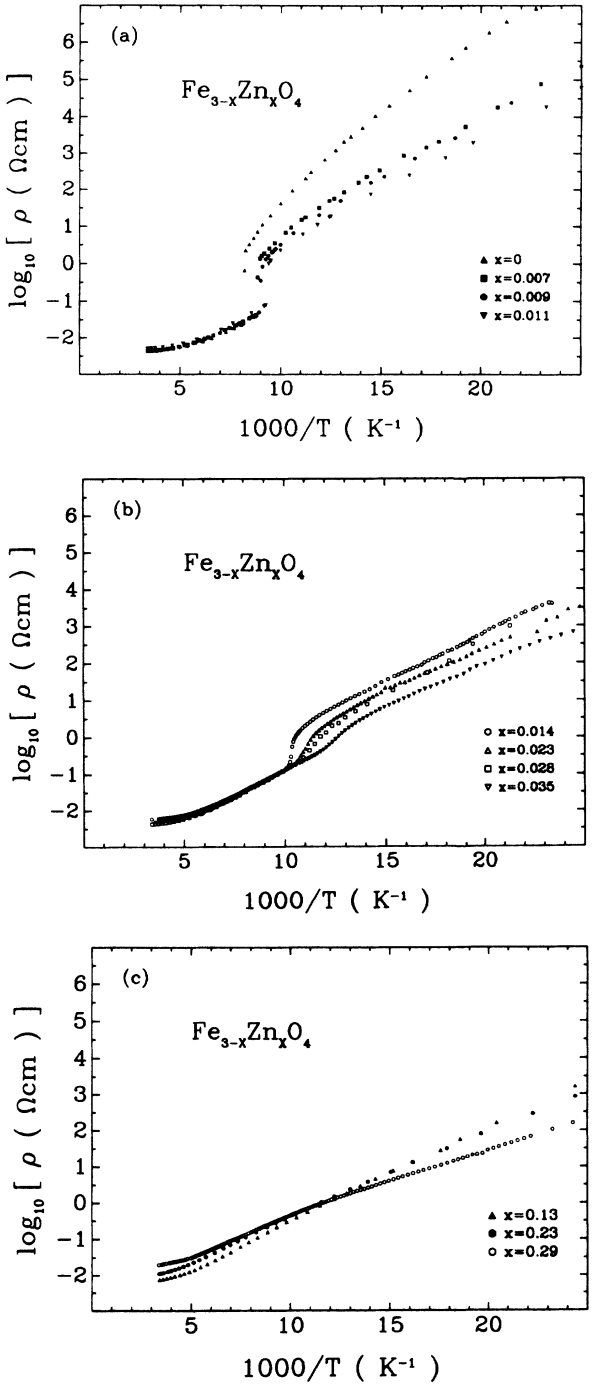

FIG. 1. Variation of resistivity of zinc ferrites with temperature, plotted as $\log_{10}\rho$ vs $1/T$. (a) $Fe_{3-x}Zn_xO_4$, with $0 \leq x \leq 0.011$, first-order regime; (b) $Fe_{3-x}Zn_xO_4$ with $0.014 \leq x \leq 0.035$, second-order regime; (c) $Fe_{3-x}Zn_xO_4$ with $0.13 \leq x \leq 0.29$, no transitions.

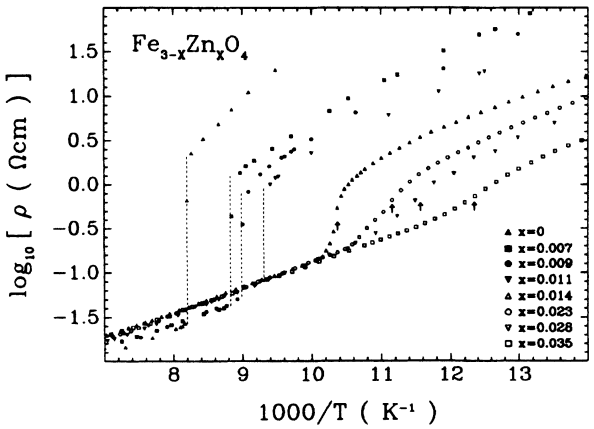

FIG. 2. Composite plot of the variation of resistivity with temperature near the Verwey transition for zinc ferrites ($Fe_{3-x}Zn_xO_4$ with $0 \leq x \leq 0.035$).

It should be noted that none of the experimental curves shown above is linear; the zinc ferrite system cannot be analyzed in terms of electrical properties of conventional semiconductors.

SEEBECK COEFFICIENT MEASUREMENTS

Seebeck coefficient measurements are entered in Figs. 3 and 4 as plots of α versus T for samples undergoing first- and second-order Verwey transitions, respectively. The following points should be noted.

(1) Peculiarities in behavior were observed in α as T was decreased below the Verwey transition temperature. For compositions in the range $0 \leq x \leq 0.035$ α passed

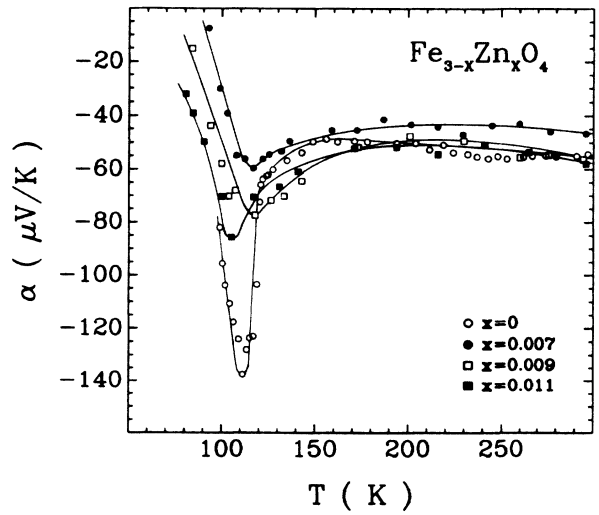

FIG. 3. Variation of Seebeck coefficient with temperature for zinc ferrites, $Fe_{3-x}Zn_xO_4$ with $0 \leq x \leq 0.011$, undergoing first-order transitions. Data cut off below 80 K; except for $x=0$ the α values for $T < T_V$ are uncertain (see the text).

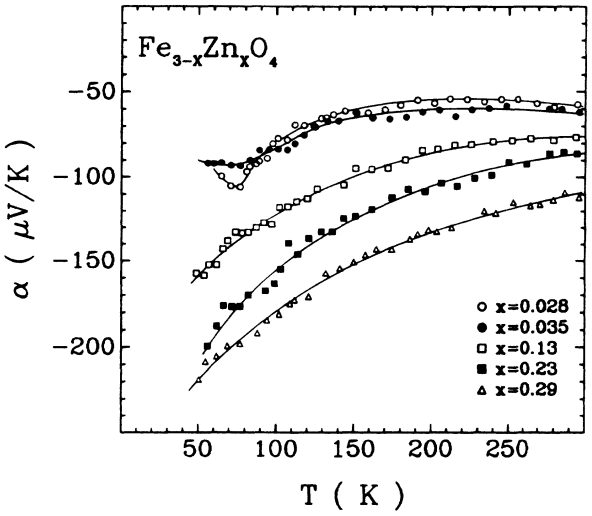

FIG. 4. Variation of Seebeck coefficient with temperature for zinc ferrites $Fe_{3-x}Zn_xO_4$ with $0.028 \leq x \leq 0.29$, undergoing second-order transitions or no transitions.

through a minimum at $T \approx T_V$, rose dramatically with a further decrease in temperature, passed through a maximum, and then diminished again. The results obtained at very low temperatures have been omitted from Figs. 3 and 4. Similar patterns were observed in our earlier runs[5,6] on undoped magnetite and in antecedent studies by Kuipers and Brabers[10,11] on undoped magnetite. The latter authors rationalized their observations on the basis of impurity effects: indeed, with the use of very high purity starting materials, the low-temperature anomalies in Fe_3O_4 could be either eliminated or at least considerably reduced.[6] We therefore arbitrarily cut off the data points for the zinc ferrite specimens below 80 to 90 K in Fig. 3 and below 50 K in Fig. 4; actually, all measurements at $T < T_V$ in Fig. 3 or below ~60 K in Fig. 4 are suspect because of the impurity problem and/or difficulties in executing the Seebeck measurements at low temperatures for samples of high resistivity.

(2) Only for pure magnetite was a real discontinuity in α seen at the Verwey transition temperature. For each of the other specimens in the series executing first-order transitions, the very slow variation of α for $T_V < T < 300$ K and the rapid change in α with $T < T_V$ produced two sets of curves that extrapolated to an intersection point near T_V. In view of comment (1) it was impossible to obtain a clear indication of a discontinuity in α at $T = T_V$ for specimens with $x > 0$.

(3) Samples undergoing a second-order Verwey transition exhibited only a small change in α with $T > T_V$ and a discontinuity in the slope of α versus T at $T = T_V$. By contrast, samples which did not suffer any transition simply showed a continuous decrease in α with diminishing T.

(4) Seebeck coefficients shown in Figs. 3 and 4 were negative; this finding cannot be readily reconciled with an elementary model in which the replacement of Fe^{3+} by Zn^{2+} adds excess holes to the pool of charge carriers.

DISCUSSION

Prior published work on the electrical properties of zinc ferrites is very limited[12–17] and confined to ceramic specimens. In the temperature and composition range where data would be intercompared there was reasonable agreement in the Seebeck coefficients obtained by previous investigators[12–14] and those shown in Fig. 4; α was invariably reported to be negative. The variation of α with x in zinc ferrites at room temperature, as reported by all investigators is in good accord. On the other hand, the resistivities of polycrystalline specimens generally changed more extensively with x and were one to three orders of magnitude above in the data set shown in Fig. 1.

In Fig. 5 we compare plots of $\log_{10}\rho$ versus $1/T$ for zinc ferrites, characterized by the stoichiometry parameter x, with plots of $\log_{10}\rho$ versus $1/T$ for nonstoichiometric single crystals of magnetite, characterized

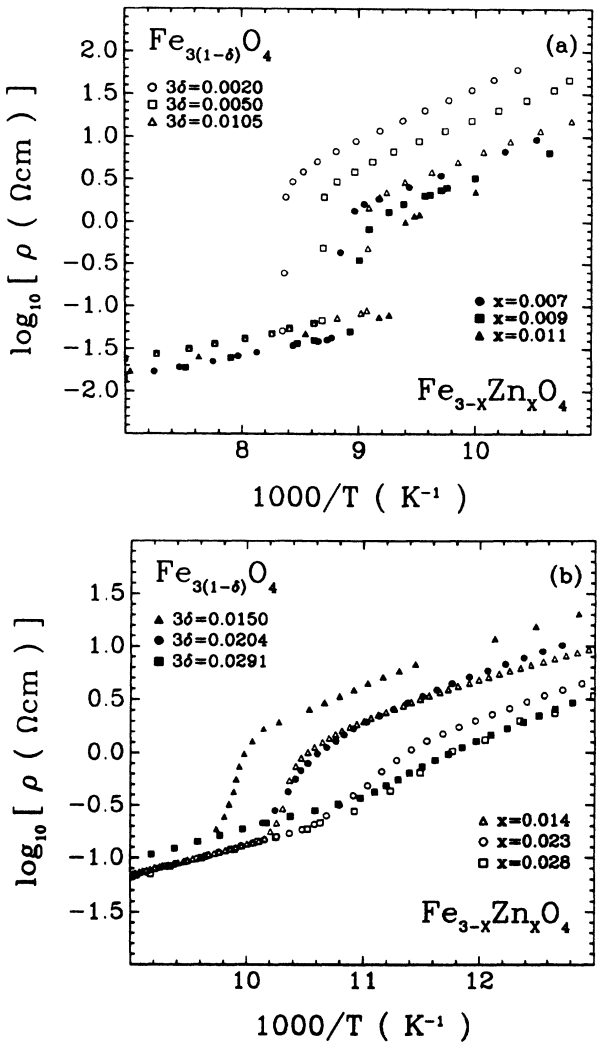

FIG. 5. Intercomparison of electrical resistivities of zinc ferrites, $Fe_{3-x}Zn_xO_4$, and nonstoichiometric magnetite, $Fe_{3(1-\delta)}O_4$ near the verwey transition temperatures. (a) Samples undergoing first-order transitions. (b) Samples undergoing second-order transitions.

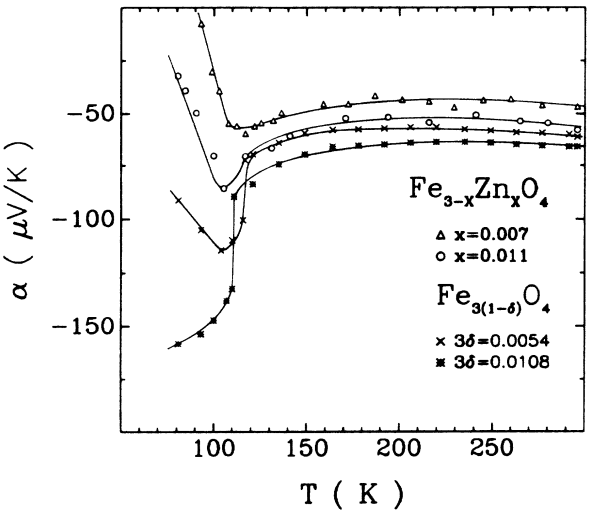

FIG. 6. Intercomparison of Seebeck coefficient with temperature for zinc ferrites $Fe_{3-x}Zn_xO_4$ and nonstoichiometric magnetite, $Fe_{3(1-\delta)}O_4$, undergoing first-order ransitions. Data cut off below 80 K.

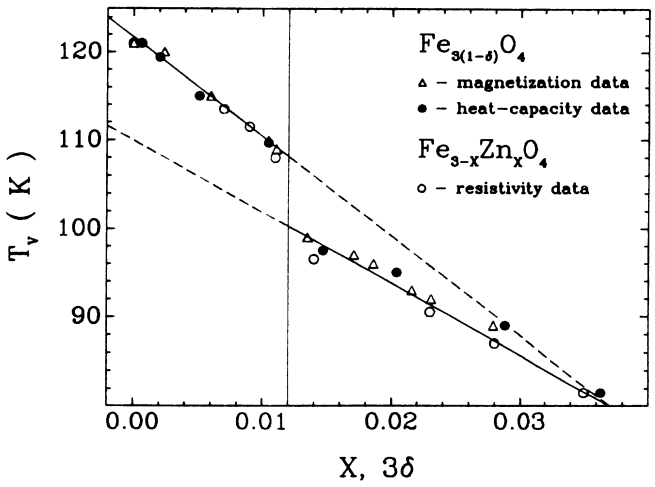

FIG. 7. Dependence of Verwey transition temperature on composition of zinc ferrites (x in $Fe_{3-x}Zn_xO_4$) or on oxygen stoichiometry of non-stoichiometric magnetite (δ in $Fe_{3(1-\delta)}O_4$).

by the parameter 3δ, which is the cation vacancy density in $Fe_{3(1-\delta)}O_4$. The obvious correspondence $x \rightleftarrows 3\delta$ is very striking. Similar results obtain for plots of α versus T which are intercompared in Fig. 6 for zinc ferrites (x parameter) and nonstoichiometric magnetite (3δ parameter).

The $x \rightleftarrows 3\delta$ correspondence may be understood on the basis of the following elementary argument: The substitution of Zn^{2+} for Fe^{3+} in the tetrahedrally coordinated (t) cation positions leads to the introduction of one hole per zinc ion on the octahedrally (o) coordinated iron ions—on the generally accepted assumptions that the remaining iron on the t sites remains exclusively in the trivalent state. In

$$Fe_{3(1-\delta)}O_4 \equiv Fe^{3+}_{2+6\delta}Fe^{2+}_{1-9\delta}O_4$$

(as determined by mass and charge balance) 6δ additional Fe^{3+} ions and 9δ fewer Fe^{2+} ions exist per formula unit than in Fe_3O_4. Thus, 3δ holes have been generated through the process of incorporating sufficient excess oxygen into magnetite to match the charge-carrier density in zinc ferrite of composition x.

The Seebeck coefficient for charge carriers in the nearly localized regime is directly related to the Fermi level which, in turn, is determined by the charge-carrier density. There should then be a close match between the two sets of Seebeck data. The superposability of α versus T plots in Fig. 6 for zinc ferrites and nonstoichiometric magnetites is a direct experimental verification of the $x \rightleftarrows 3\delta$ correspondence. Similar statements apply to the resistivity data shown in Fig. 5. It is remarkable, however, that not only the charge-carrier densities but also the mobilities of the holes in the zinc ferrites must be comparable to those of the nonstoichiometric magnetites; otherwise, the superposition of the resistivity data, subject to the correspondence $x \rightleftarrows 3\delta$, would not hold.

We show in Fig. 7 the change of the Verwey transition temperature T_V with x and 3δ. The data for nonstoichiometric magnetite are based on heat capacity[2–4] and magnetization[7,8,18] measurements; the entries for zinc ferrites are based on the resistivity studies. As is seen, measurements for the two types of materials superpose very well under the assumed $x \rightleftarrows 3\delta$ correspondence. The scatter of the data for the second-order regime $x_c \le x \le 3x_c$ is greater than for the first-order regime $0 \le x_c < x_c$ because judgmental factors in the assignment of T_V play a much greater role in the former than in the latter regime. Lastly, we show in Fig. 8 a logarithmic plot of the size of changes in resistivity at the Verwey transition against x and 3δ for samples undergoing both a first-order or a second-order transition. In the latter case an extrapolation procedure was used. Once again the results for zinc ferrites and nonstoichiometric magnetite superpose very well. Thus, the electrical properties of both

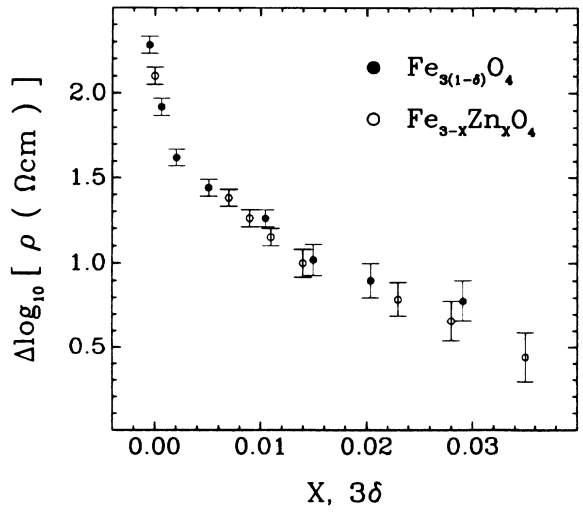

FIG. 8. Variation of the change of resistivity at the Verwey transition of zinc ferrites, $Fe_{3-x}Zn_xO_4$, with composition x or with oxygen stoichiometry, 3δ, of magnetite, $Fe_{3(1-\delta)}O_4$.

the low- and high-temperature phases of the two classes of materials are very similar.

In view of the above features the theoretical analysis concerning the electrical properties of the zinc ferrites can be clearly modeled on the earlier treatment of nonstoichiometric magnetite.[19–22] A brief outline suffices; we also correct a number of earlier technical errors.

The zinc ferrite system is simulated, in a manner analogous to $Fe_{3(1-\delta)}O_4$, by a two-level system of energies ε_0 and ε_1 and corresponding degeneracies g_0 and g_1. We set $\varepsilon_0=0$ and write $\varepsilon_1=\varepsilon\psi-\frac{1}{2}\lambda\psi^2$, where ψ is an order parameter.

The dependence of ε_1 on ψ allows for electron correlation effects through the term $\lambda\psi^2/2$; ε and λ are two parameters that must be specified in their dependence on $x=3\delta$ by a fitting routine described in detail elsewhere.[19,21] For the first-order (second-order) regime it is appropriate to select $g_1=2$, $g_0=1$ ($g_1=g_0=2$). The order parameter is found through numerical solution of the equilibrium constraint

$$(\varepsilon-\lambda\psi)/k_BT=\ln[(g_1/g_0)(1-\psi)/\psi] , \tag{1}$$

in which k_B is the Boltzmann constant.

The Fermi level is then obtained through the balance-of-carriers expression

$$\frac{1-x}{2}=\frac{g_1\psi}{1+\exp(\mu/k_BT)}+\frac{g_0(1-\psi)}{1+\exp\{[-(\varepsilon-\lambda\psi)+\mu]/k_BT\}} . \tag{2}$$

Having solved numerically for μ one may specify the Seebeck coefficient as

$$\alpha=-\frac{\varepsilon-\lambda\psi}{eT}-\frac{\mu}{eT} , \tag{3}$$

where e is the electronic charge.

The electrical conductivity is given by

$$\sigma=n_c eu , \tag{4}$$

where the charge-carrier density is specified as

$$n_c=(2)g_1\psi/[1+\exp(\mu/k_BT)] . \tag{5}$$

In Eq. (4) the mobility in the small-polaron regime is

$$u=\frac{g_0(1-\psi)}{1+\exp\{[-(\varepsilon-\lambda\psi)+\mu]/k_BT\}}\frac{ea^2\Gamma}{k_BT} , \tag{6}$$

where a is the jump distance (o-o site separation). The polaron jump rate Γ is specified by the Arrhenius law

$$\Gamma=P\nu_0\exp(-\varepsilon/k_BT) , \tag{7}$$

where ν_0 is the appropriate optical polaron frequency and P is a probability factor for electron transfer after the polarization displacement has taken place.

The fit of the above theory to the electron properties of $Fe_{3(1-\delta)}O_4$ was found to be satisfactory; hence, the same is found to be the case for $Fe_{3-x}Zn_xO_4$. Several additional comments are appropriate.

(i) The fact that α is negative may be understood on the basis of the following argument:[20–22] We show in Fig. 9 the variation on ε_0, ε_1, and μ with temperature for the illustrative case of stoichiometric magnetite for which $\varepsilon/k_B=349$ K, $\lambda/k_B=531$ K. One notices that for $T<T_V$, $\varepsilon_0=0$, ε_1 varies roughly parabolically with T, and $\mu\ll\varepsilon_1$ over the entire temperature range. Thus $\varepsilon_1-\varepsilon_0\equiv\varepsilon-\lambda\psi$ dominates; $(\varepsilon-\lambda\psi)/T$ as well as α should therefore be nearly linear in $T<T_V$, as is found to be the case experimentally. Again, we neglect the irregularity of behavior in α for $T\ll T_V$, where extraneous effects enter. For $T>T_V$, $\varepsilon_1-\varepsilon_0\ll\mu$; $\mu<0$, which diminishes roughly linearly with increasing T, thus dominates, and $\alpha\sim-\mu/T$ is roughly constant, in agreement with experimental results. Similar observations hold for all other $Fe_{3-x}Zn_xO_4$ samples, except that for $x>x_c$ the discontinuities in ε_1 or μ are replaced by discontinuities in their slope. Overall, there is reasonable agreement between the observed electrical properties and those calculated on the basis of the above model.

It is difficult to conceive that valence fluctuations can occur at or below room temperature among the zinc and ferric ions located in the tetrahedral interstices. Accordingly, it is likely that charge transport will occur solely via valence fluctuations among iron ions on the octahedral sites, possibly aided by superexchange via intervening oxygen ions. This assumption is in accord with the experimental observation concerning the similarity in electrical properties of $Fe_{3-x}Zn_xO_4$ and $Fe_{3(1-\delta)}O_4$.

(iii) The fact that the electron mobility in nonstoichiometric magnetite is very close to that of zinc ferrite of comparable composition is remarkable and leads to two possible deductions: Either the charge-carrier vacancies occur almost exclusively on the cation sublattice

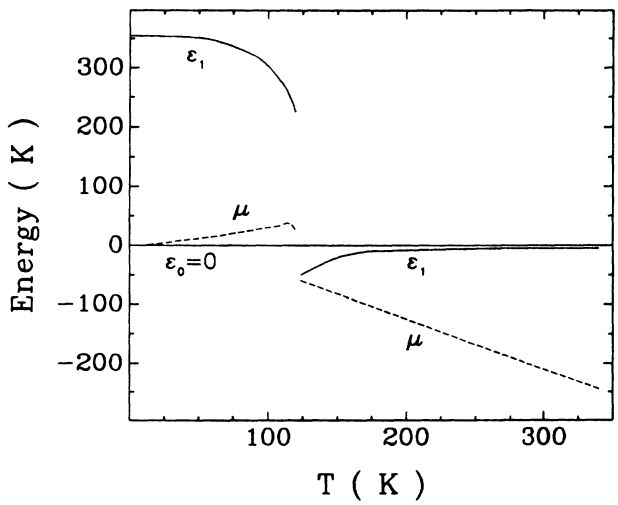

FIG. 9. Variation of energy and Fermi level in stoichiometric magnetite with temperature. Zero of energy coincides with ε_0. Solid curve: variation of ε_1 with T. Dashed curve: variation of Fermi level with T. Break in curves occur at Verwey transition temperature of 121 K.

located on the tetrahedral interstices. Or, the vacancies are also distributed on sites normally occupied by octahedral cations without affecting the charge-carrier mobilities significantly. This latter possibility is not unlikely: it is well established that lattice vacancies function as traps for charge carriers, frequently with a shallow binding energy of the order of 50–300 K. In such circumstances charge carriers drifting under the influence of an applied electric field may be trapped at vacancies for times comparable to their residence time on cations.

CONCLUSION

We have provided evidence showing that the electrical properties and Verwey transition temperatures of $Fe_{3-x}Zn_xO_4$ are quite similar to those of $Fe_{3(1-\delta)}O_4$, with the correspondence $x \rightleftarrows 3\delta$. These findings are rationalized on the basis of an elementary model. The data suggest that conduction occurs by charge transport involving valence fluctuations on cations in octahedral locations and that any cation vacancies present at those sites do not greatly impede the transport process.

ACKNOWLEDGMENTS

Very stimulating discussions with Q. W. Choi, J. Koenitzer, and J. Spałek are gratefully acknowledged. This research was supported on National Science Foundation (NSF) Grant No. DMR 86-16533 A02.

*Present address: Shanghai Institute of Ceramics, Academia Sinica, Shanghai 200050, People's Republic of China.

†On leave from Akademia Górniczo-Hutnicza, Kraków, Poland.

[1]R. Aragón, D. J. Buttrey, J. P. Shepherd, and J. M. Honig, Phys. Rev. B **31**, 430 (1985).

[2]J. P. Shepherd, J. W. Koenitzer, R. Aragón, C. J. Sandberg, and J. M. Honig, Phys. Rev. B **31**, 1107 (1985).

[3]R. Aragón, J. P. Shepherd, J. W. Koenitzer, D. J. Buttrey, R. J. Rasmussen, and J. M. Honig, J. Appl. Phys. **57**, 3221 (1985).

[4]J. P. Shepherd, R. Aragón, J. W. Koenitzer, and J. M. Honig, Phys. Rev. B **32**, 1818 (1985).

[5]R. Aragón, R. J. Rasmussen, J. P. Shepherd, J. W. Koenitzer, and J. M. Honig. J. Magn. Mater. **54-57**, 1335 (1986).

[6]R. J. Rasmussen, R. Aragón, and J. M. Honig, J. Appl. Phys. **61**, 4395 (1987).

[7]Z. Kąkol and J. M. Honig, Solid State Commun. **70**, 967 (1989).

[8]Z. Kąkol and J. M. Honig, Phys. Rev. B **40**, 9090 (1989).

[9]P. Wang, M. W. Wittenauer, D. J. Buttrey, Q. W. Choi, P. Metcalf, Z. Kąkol, and J. M. Honig (unpublished).

[10]A. J. M. Kuipers and V. A. M. Brabers, Phys. Rev. B **14**, 1401 (1976).

[11]A. J. M. Kuipers and V. A. M. Brabers, Phys. Rev. B **20**, 594 (1979).

[12]A. A. Samokhvalov and A. G. Rustamov, Fiz. Tverd. Tela **7**, 1198 (1965) [Sov. Phys.—Solid State **7**, 961 (1965)].

[13]B. Gillot, R. M. Benloucif, and A. Rousset, Phys. Status Solidi A **65**, 205 (1981).

[14]G. Srinivasan and C. M. Srivastava, Phys. Status Solidi B **103**, 665 (1981).

[15]B. Gillot, Phys. Status Solidi A **69**, 719 (1982).

[16]B. Gillot and F. Jemmali, Phys. Status Solidi A **76**, 601 (1983).

[17]M. A. Mousa and M. A. Ahmed, J. Mater. Sci. **23**, 3083 (1988).

[18]Z. Kąkol, R. N. Pribble, and J. M. Honig, Solid State Commun. **69**, 793 (1989).

[19]R. Aragón and J. M. Honig, Phys. Rev. B **37**, 209 (1988).

[20]J. M. Honig and R. Aragón, Physica B **150**, 129 (1988).

[21]J. M. Honig, Phys. Chem. Miner. **15**, 476 (1988).

[22]J. M. Honig and P. Gopalan, Solid State Ionics **32-33**, 802 (1989).